J|A|C|S COMMUNICATIONS

Published on Web 05/28/2009

Heteroepitaxial Ferroelectric $ZnSnO_3$ Thin Film

Jong Yeog Son, Geunhee Lee, Moon-Ho Jo, Hyungjun Kim, Hyun M. Jang, and Young-Han Shin*

Department of Materials Science and Engineering and Division of Advanced Materials Science, Pohang University of Science and Technology, Pohang, Korea

Received April 20, 2009; E-mail: yhshin@postech.ac.kr

Since the discovery of ferroelectricity in 1920 by Valasek, ferroelectric materials have been widely investigated due to their various physical properties including spontaneous polarization, piezoelectric strain, and piezoelectricity.[1−5] Interestingly, the fabrication technique of ferroelectric thin films enables design of integrated ferroelectric circuits for nonvolatile random access memory (NVRAM).[6−9] Pb-based ferroelectric thin films such as $Pb(Zr,Ti)O_3$ (PZT) have been extensively deliberated as feasible ferroelectric media because they show high ferroelectric polarization although the Pb element brings about environmental pollution.[1,6,7] PZT ceramics have been attractively used for the application of piezoactuators in microelectromechanical systems such as a scanning probe microscope.[10,11] Meanwhile, many researchers have attempted to substitute Pb-based ferroelectric thin films for new ferroelectric materials such as Bi-based perovskite oxides.[8,9,12−15] Layered perovskite oxides such as $SrBi_2Ta_2O_9$ exhibited good endurance for fatigue while showing a smaller ferroelectric polarization than Pb-based ferroelectric thin films.[5] Since the fatigue problem is easily overcome by using oxide electrodes such as IrO_2 and RuO_2, it is more necessary to improve ferroelectric polarization in new lead-free ferroelectric thin films for the application of NVRAMs.[6,16]

Recently, Inaguma et al. reported that $ZnSnO_3$ which was synthesized with a high-pressure synthesis method could be possibly used for lead-free ferroelectrics due to its quite large polarization.[15] Yet, they only discussed that a novel polar $LiNbO_3$-type oxide $ZnSnO_3$ had a possibility of high ferroelectric polarization. Here, we experimentally demonstrated a high ferroelectric polarization of $\sim$47 $\mu C/cm^2$ in a heteroepitaxial $ZnSnO_3$ thin film. To understand the experimental data at the microscopic atomic level, we performed first-principles density-functional calculations.

We fabricated a heteroepitaxial $ZnSnO_3$ thin film on a (111) $SrRuO_3$/(111) $SrTiO_3$ substrate by pulsed laser deposition (PLD) with a Nd:YAG laser (355 nm, $\sim$2 J/cm^2). For preparation of the $SrRuO_3/SrTiO_3$ substrate, a $SrRuO_3$ thin film was deposited on a single crystalline (111) $SrTiO_3$ substrate which was etched in a buffered HF solution and annealed in oxygen ambient at 1000 °C for the formation of well-defined terraces. To prepare a ceramic $ZnSnO_3$ target, a stoichiometric mixture of ZnO (Aldrich 99.999%) and SnO_2 (Aldrich 99.995%) was ground and pressed into pellets. The pellets were calcined at 850 °C for 10 h and then reground, pressed into pellets, and sintered by hot isostatic pressing (high-pressure annealing) at 1000 °C in a high oxygen partial pressure of 5 GPa for 12 h. After the base pressure reached 5×10^{-7} Torr, the substrate temperature was set to 700 °C with an oxygen partial pressure of 200 mTorr during the deposition of a $ZnSnO_3$ thin film. The structure of the $ZnSnO_3$ thin film was investigated with X-ray diffraction (XRD, Cu Kα radiation 1.542 Å). The tentative composition of the $ZnSnO_3$ thin film was obtained by using energy dispersive X-ray spectroscopy (EDS) and auger electron spectroscopy (AES). The thickness of the thin film was 100 nm obtained by a cross-sectional view by scanning electron microscopy (SEM). The surface morphology and the roughness of the $ZnSnO_3$ thin film were observed by atomic force microscopy (AFM). We fabricated a Pt top electrode in a circular form (diameter, 100 μm) with a thickness of 100 nm on the thin film by using a shadow mask and RF magnetron sputtering. These Pt top electrodes were annealed at 400 °C for 5 min. Ferroelectric hysteresis loops were measured using an RT66A (Radiant Technologies, Inc.) test system.

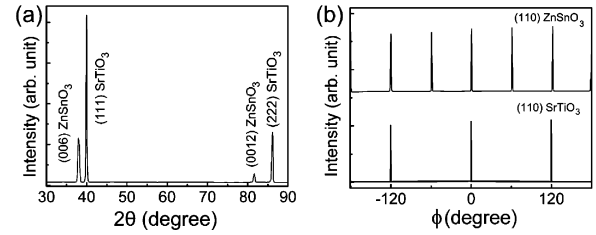

Figure 1. (a) X-ray diffraction pattern of the epitaxial (111) $ZnSnO_3$ thin film. (b) Φ scans of the (110) peaks of $ZnSnO_3$ and (110) peaks of the $SrTiO_3$ substrate.

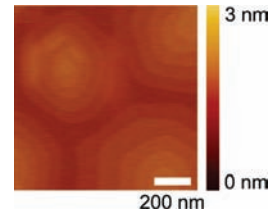

Figure 2. AFM image of the epitaxial (111) $ZnSnO_3$ thin film. Multiterraces are clearly observed, indicating a layer-by-layer growth mode.

The XRD pattern of the $ZnSnO_3$ thin film on the (111) $SrRuO_3$/(111) $SrTiO_3$ substrate is shown in Figure 1. In the $\theta-2\theta$ scan, only (006) and (0012) peaks were observed, indicating a possibility of epitaxial growth of the $ZnSnO_3$ thin film. The full widths at half-maximum (FWHMs) of (006) and (0012) peaks are $\sim$0.5° and 0.6°, respectively. We also measured rocking curves for the (006) and (0012) peaks, in which the FWHMs of the (006) and (0012) peaks are equal to 0.9° and 1.1°, respectively. These small FWHMs of rocking curves indicate good crystallinity of the $ZnSnO_3$ thin film along the out-of-plane orientation. Although there is a lattice misfit of $\sim$5% between the $ZnSnO_3$ thin film and the (001) $SrRuO_3$ bottom electrode, the thin film exhibits a highly crystallized structure. From the (001) and (002) peaks of the $ZnSnO_3$ thin film, we estimated a *c*-lattice constant of 13.87 Å, which is shorter than the bulk lattice constant of 14.00 Å.

To check the in-plane orientation, we performed Φ-scans for the (110) peak of the $ZnSnO_3$ thin film and the (110) peak of the (111) single crystal $SrTiO_3$ substrate [Figure 1b]. The (110) peak of the (111) single crystal $SrTiO_3$ substrate shows 3-fold symmetry while the (110) peak of the $ZnSnO_3$ thin film has 6-fold symmetry. This 6-fold symmetry means that the thin film has twin defects.

10.1021/ja903133n CCC: $40.75

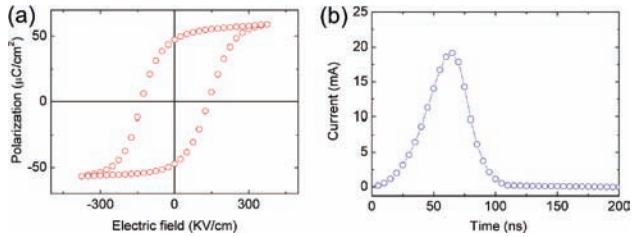

Figure 3. (a) $P-E$ hysteresis loops of the epitaxial (111) $ZnSnO_3$ thin film. A remanent polarization is ~47 $\mu C/cm^2$. (b) Switching current as a function of time for the epitaxial (111) $ZnSnO_3$ thin film under a switching bias of 5 V. The fast switching behavior is within 100 ns.

The relative positions of the in-plane peaks in Figure 1b reveal that the $ZnSnO_3$ thin film was epitaxially grown, and the pseudocubic [111] directions of the $ZnSnO_3$ thin film and the $SrTiO_3$ substrate are parallel to the out-of-plane orientation. This indicates that the $ZnSnO_3$ thin film has a heteroepitaxial growth on the $SrTiO_3$ substrate. The FWHM of the (110) rocking curve is ~0.6°, indicating the well-defined crystallinity of the $ZnSnO_3$ thin film along the in-plane orientation. From the (002) and (110) peaks, we could estimate the a-lattice constant of 5.34 Å which is larger than the bulk lattice constant of 5.26 Å.

By observing the surface morphology of the $ZnSnO_3$ thin film with AFM, we found that large terraces with a width of ~1000 Å were formed on the film following the step flow growth mechanism, which represents that adatoms on the surface diffuse easily.[17] The root-mean-square roughness is ~0.6 nm over the 1 μm × 1 μm scan area [Figure 2].

To investigate the ferroelectric property of the $ZnSnO_3$ thin film, we observed a hysteresis loop of the Pt/$ZnSnO_3$/$SrRuO_3$ capacitor at a measurement frequency of 10 kHz. The Pt/$ZnSnO_3$/$SrRuO_3$ capacitor exhibits a high remanent polarization of 47 $\mu C/cm^2$ ($2P_r \approx 94\ \mu C/cm^2$) with a coercive electric field of ~130 kV/cm [Figure 3a]. The saturation polarization is ~58 $\mu C/cm^2$ which is slightly larger than the remanent polarization, indicating a high crystalline structure of epitaxial $ZnSnO_3$ thin film. We also checked hysteresis loops of the Pt/$ZnSnO_3$/$SrRuO_3$ capacitor at various measurement frequencies in the range 1 kHz−1 MHz. The coercive electric field increased with the measurement frequency (see Supporting Information, SI). In addition, we measured the switching current with a square pulse of 5 V (rising time of ~1 ns). The Pt/$ZnSnO_3$/$SrRuO_3$ capacitor shows a fast switching behavior with a switching time of 100 ns [Figure 3b].

To investigate the atomic view of polarization in hexagonal $ZnSnO_3$, we performed first-principles calculations with the Vienna Ab initio Simulation Package (VASP).[18] The exchange and correlation energies of electrons were carried out within a local density approximation (LDA), and the interactions between ions and electrons were described by the projector augmented wave (PAW) potentials. The calculated lattice constants are $a = 5.24$ Å and $c = 13.88$ Å with a cell volume of 54.92 Å^3 per formula unit cell (Table S1, SI). We evaluated the ionic displacements of Zn and Sn relative to the oxygen octahedral center [Figure 4]. The A cation (Zn) displacement (0.55 Å) was larger than the B cation (Sn) displacement (0.21 Å), which is due to the larger space of the A site for the Zn atom to move: the covalent radius of Zn (1.31 Å) is smaller than that of Sn (1.41 Å). Using the Berry phase approach,[19,20] we calculated polarization of 60 $\mu C/cm^2$ along the pseudocubic [111] direction, which is comparable with our experimental value as well as the result of the analytic calculation with the ionic displacements and the atomic valences.[15]

In summary, we fabricated an epitaxial $ZnSnO_3$ thin film by PLD and carried out X-ray and AFM studies to investigate its structural and ferroelectric behaviors. The heteroepitaxial thin film showed a hexagonal structure with slightly elongated a-lattice and shrunken c-lattice constants. We obtained a high ferroelectric polarization of ~47 $\mu C/cm^2$ for the film, which gives a new approach for the substitution of Pb-based ferroelectric thin films.

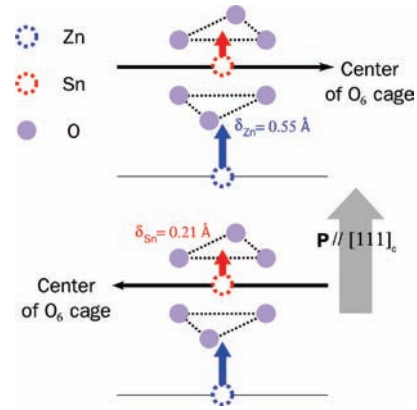

Figure 4. Ionic displacements of Zn and Sn in the $R3c$ phase of $ZnSnO_3$ with polarization aligned along the $[111]_c$ direction. The Sn displacement is defined as the distance between the center of the oxygen octahedral cage and the Sn ion in this cage, and the Zn displacement as the distance between the center of two neighbor oxygen octahedral cages and the Zn between the cages along the $[111]_c$ direction.

Acknowledgment. This work was supported by BK21 project 2009, Korea Research Foundation Grants No. KRF-2008-313-C00252 and No. KRF-2008-313-C00258, and the WCU program by MEST (Grant No. R31-2008-000-10059-0).

Note Added after ASAP Publication. The version published May 28, 2009 contained an error in the seventh paragraph. The corrected version was published June 17, 2009.

Supporting Information Available: Frequency dependence of polarization and structural data. This material is available free of charge via the Internet at http://pubs.acs.org.

References

(1) Scott, J. F.; PazDeAraujo, C. A. *Science* **1989**, 246.
(2) Orlando, A.; James, F. S.; Ramamoorthy, R. *Phys. Today* **1998**, *51*, 22–27.
(3) Dawber, M.; Rabe, K. M.; Scott, J. F. *Rev. Mod. Phys.* **2005**, *77*, 1083.
(4) Valasek, J. *Phys. Rev.* **1921**, *17*, 475.
(5) de Araujo, C. A. P.; Cuchiaro, J. D.; McMillan, L. D.; Scott, M. C.; Scott, J. F. *Nature* **1995**, *374*, 627–629.
(6) Takashi, N.; Yuichi, N.; Akira, K.; Hidemi, T. *Appl. Phys. Lett.* **1994**, *65*, 1522–1524.
(7) Noheda, B.; Gonzalo, J. A.; Cross, L. E.; Guo, R.; Park, S. E.; Cox, D. E.; Shirane, G. *Phys. Rev. B* **2000**, *61*, 8687.
(8) Son, J. Y.; Kim, B. G.; Kim, C. H.; Cho, J. H. *Appl. Phys. Lett.* **2004**, *84*, 4971–4973.
(9) Son, J. Y.; Park, C. S.; Shin, Y. H. *Appl. Phys. Lett.* **2008**, *92*, 222911–3.
(10) Binnig, G.; Quate, C. F.; Gerber, C. *Phys. Rev. Lett.* **1986**, *56*, 930.
(11) Muralt, P. J. *Micromech. Microeng.* **2000**, *10*, 136–146.
(12) Wang, J.; Neaton, J. B.; Zheng, H.; Nagarajan, V.; Ogale, S. B.; Liu, B.; Viehland, D.; Vaithyanathan, V.; Schlom, D. G.; Waghmare, U. V.; Spaldin, N. A.; Rabe, K. M.; Wuttig, M.; Ramesh, R. *Science* **2003**, *299*, 1719–1722.
(13) Zylberberg, J.; A. Belik, A.; Takayama-Muromachi, E.; Ye, Z.-G. *Chem. Mater.* **2007**, *19*, 6385–6390.
(14) Cho, J. H.; Bang, S. H.; Son, J. Y.; Jia, Q. X. *Appl. Phys. Lett.* **1998**, *72*, 665–667.
(15) Inaguma, Y.; Yoshida, M.; Katsumata, T. *J. Am. Chem. Soc.* **2008**, *130*, 6704–6705.
(16) Al-Shareef, H. N.; Bellur, K. R.; Auciello, O.; Kingon, A. I. *Thin Solid Films* **1995**, *256*, 73–79.
(17) Burton, W. K.; Cabrera, N.; Frank, F. C. *Philos. Trans. R. Soc. London, Ser. A* **1951**, *24*, 299.
(18) Kresse, G.; Joubert, D. *Phys. Rev. B* **1999**, *59*, 1758.
(19) King-Smith, R. D.; Vanderbilt, D. *Phys. Rev. B* **1993**, *47*, 1651.
(20) Resta, R. *Rev. Mod. Phys.* **1994**, *66*, 899–915.

JA903133N